INVESTIGATION OF THE INTERMEDIATE NEUTRON CAPTURE ON UNSTABLE NUCLIDES BY MEANS OF THE ACTIVATION METHOD

V. Skorkin[1], P. Mastinu[2]

[1]Institute for Nuclear Research RAS, Moscow, Russia
[2]Istituto Nazionale di Fisica Nucleare, Laboratori Nazionali di Legnaro, Italy

Abstract

The statistical uncertain of the Maxwellian-averaged neutron capture cross sections measuring by the activation method was calculated for more than 20 unstable nuclides from strontium to hafnium at the stellar thermal energy of kT=30 keV. The samples of unstable nuclides (0.02-2 μg mass) can be produced by ion implantation of Radioactive Ion Beam into a graphite target. The unstable isotopes can be activated by irradiating neutrons with a Maxwellian-shaped neutron spectrum from a lithium target. After the irradiation unstable nuclide activity can be measured with using two HPGe detectors or BriLanCe detectors.

1 Intradaction

Accurate knowledge of neutron-nucleus reaction cross sections in the keV region is of primary importance in studies of stellar nucleosynthesis and in applications of nuclear technology for determines the amount of radionuclides in burnt fuel elements of fast reactors.

Proton-induced nuclear reactions determine the nucleosynthesis of light elements in a variety of stellar objects in the universe. Three different processes can be identified in a mass region of the chemical elements heavier than iron, the slow (***s***) neutron capture process during stellar helium burning, the rapid (***r***) neutron capture process, and the photo-dissociation (***p***) process, the latter two being presumably related to Supernova explosions.

About half of the elemental abundances between Fe and Bi are produced by the s-process, which is characterized by relatively low neutron densities (10^{11} neutron/cm^{2}s^{-1}) and neutron capture times, which are typically much longer than the half-lives against beta-decay. Some unstable nuclei act as branching points in the reaction path of the ***s***- process (Fig.1).

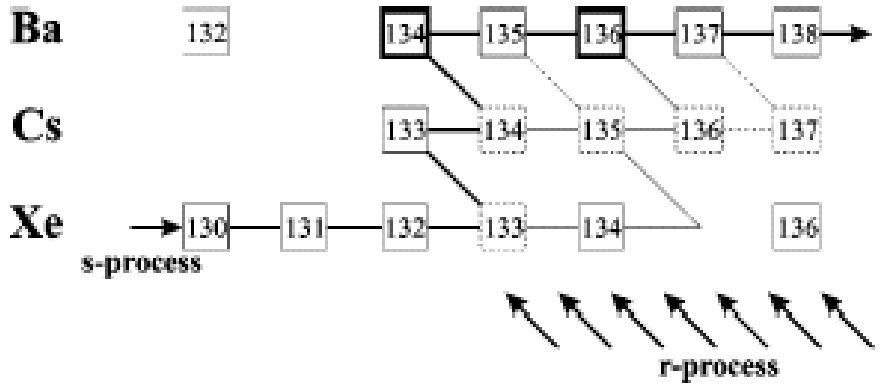

Fig. 1. The ***s***-process path in the Xe-Cs-Ba region, which includes the important branching point ^{134}Cs. This branching determines the isotopic ratio of the isotopes ^{134}Ba and ^{136}Ba [1].

The neutron capture cross section data are the fundamental ingredient for the calculation of the stellar reaction rates. The abundances of the produced isotopes are inversely proportional to their neutron capture cross sections.

The relevant cross sections can be measured directly using radioactive ion beams.

2 Experimental procedure

The stellar *s*-process models require Maxwellian -averaged capture cross sections (MACS) of unstable nuclei of over a temperature range from kT=1 keV to kT=100 keV.

$$\frac{\langle \sigma v \rangle}{v_T} = \frac{2}{\sqrt{\pi}} \frac{\int_0^\infty \sigma(E_n) E_n \exp(-E_n/kT) dE_n}{\int_0^\infty E_n \exp(-E_n/kT) dE_n} \quad (1)$$

Measurements of the MACS usually carried out at Time of Flight facilities (TOF) with mass sample to the milligrams. The accurate MACS can be obtained by the neutron activation analysis (NAA) providing neutrons with the stellar spectrum. This technique offers the high sensitivity, which is essential since measurements on radioactive isotopes have to be carried out with very small samples (≤ 1 μg).

The samples of unstable nuclides (10^{14}-10^{16} atoms) can be produced by ion implantation of Radioactive Ion Beam (RIB) into a graphite target. The RIB (10^{10} s^{-1} intensity) will be available at SPES (Selective Production of Exotic Species) project at Laboratori Nazionali di Legnaro, Italy [2]. The project based on a superconductive accelerator complex included Primary Linac accelerating protons to an energy of 5 MeV with a current of 20 mA c.w. and Secondary Linac that will operate in pulsed mode at a repetition rate of 50 HZ and a duty cycle of 1% with an average current of 0.2 mA.

The primary proton beam used for production of fission fragments (10^{13} s^{-1}) from a uranium like-target by means of a neutron converter. Neutron rich ion species are extracted, selected, further ionized at high charge state, isotopically purified and then accelerated through a Secondary Linac at energies up to 15 MeV/A.

In this project, neutron generation is proposed to be carried out by dropping an intensive proton beam onto lithium target using ^{7}Li(p,n)^{7}Be threshold reaction and a good approximation to a Maxwellian-shaped neutron spectrum (MSNS) at 30 keV can be obtained by shaping the proton beam energy (Fig. 2).

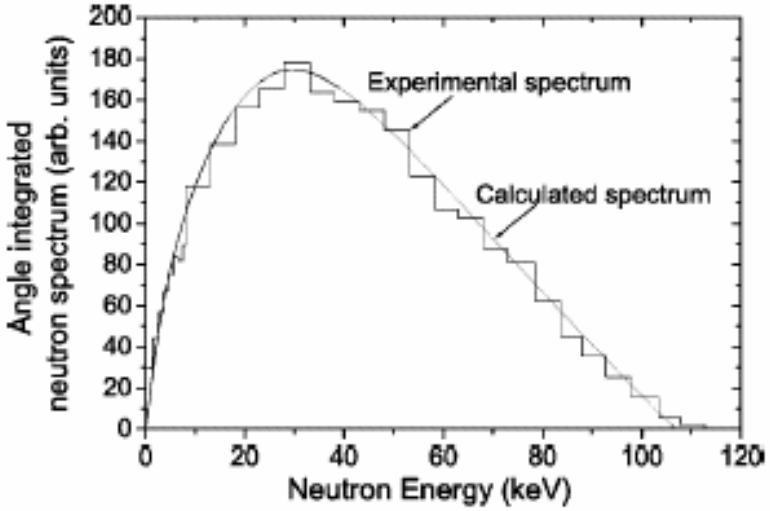

Fig. 2. The MSNS of the epithermal neutrons from the lithium target [3].

The monochromatic proton beam can be shaped by means of a 34 mg/cm^2 thickness rotating carbon foil, reducing and spreading its 5 MeV energy to 1.712 ± 0.09 MeV. The epithermal neutrons with MSNS at *kT*=30_for experiment can be produced by a part of protons (4.4%) with the energy above the reaction threshold energy (1881 keV). The sample, contained unstable isotopes can be activated by irradiating neutrons with the flux of the order of $5.3 \cdot 10^{10}$ neutron/cm^2·s.

In the second project neutrons with maximum energy board of 400 keV are produced by spallation reactions induced by a pulsed, 1-160 μs wide and repetition rate up to 50 Hz, 209 MeV/*c* proton Linac at INR RAS beam with up to 12 mA current per pulse, impinging on a tungsten or lead target. Spallation reaction results in emission of fast neutron flux up to of 10^{15} n/s from the target. A system of converters and filters modify a wide energy spectrum to the MSNS at a Spectrometer for neutrons slowing down in lead (LNS-100) and an Irradiation facility (RADEX). Density of epithermal neutrons flux with energy from 1 keV to 100 keV
in the irradiated channels can reach up to 10^{12} n·cm^{-2}·s^{-1}.

The samples containing unstable nuclides can be obtained from RFNC – VNIIEF [4].

3 Measurement procedure

After the irradiation the samples containing unstable nuclides can be accommodated close in front of two high-purity germanium HPGe or BriLanCe ($LaBr_3$:Ce) detectors to measure a induced gamma activity of activated nuclides (Fig. 3).

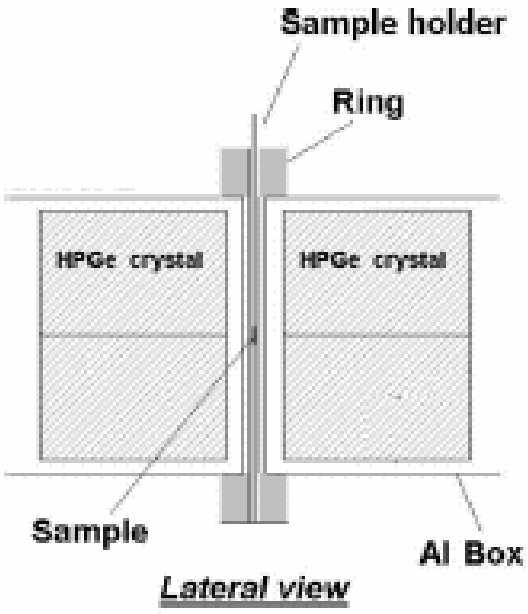

Fig. 3. Setup of the HPGe detectors. The close geometry requires an exact and reproducible positioning of sample and detectors, which was achieved with a special sample holder.

This characteristics of the HPGe, BrilanCe detectors are given in Table 1.

The background should be reduced by a lead shielding.

The neutron capture cross section of the unstable isotopes can be measured relative to that of gold (^{198}Au, Half-life 2.7 d, gamma 411.8 keV energy). The extrapolation stellar cross section of gold is yields 582± 9 mb at stellar temperature kT=30 keV.

Table.1. Characteristics of **HPGe** (2"×3"), **BrilanCe B380)** (3"×3") and **NaI(Tl))(3"×3")** detectors.

Energy of γ- rays, keV	**122**(^{57}Co)	**356**(^{113}Sn)	**662**(^{137}Cs)	**882**(^{54}Mn)	**1332**(^{60}Co)	**2615**
Detector						
HPGe						
Resolution	**1.0keV**	**1.2keV**	**1.3keV**	**1.5keV**	**1.7keV**	
Efficiency (c_{max}=1.5·10^5 s^{-1})	**0.4**	**0.16**	**0.09**	**0.07**	**0.05**	
B380(LaBr$_3$)						
Resolution	**6.6%**	**3.8%**	**2.9%**	**2.6%**	**2.1%**	**1.6%**
Efficiency (c_{max}= 8·10^5 s^{-1})	**0.84**	**0.48**	**0.36**	**0.25**	**0.22**	**0.085**
NaI(Tl)						
Resolution	**8.9%**	**9.1%**	**7.0%**	**6.4%**	**5.4%**	**4.5%**
Efficiency	**0.8**	**0.45**	**0.3**	**0.2**	**0.15**	**0.053**

c_{max} – The maximum count rate for this detector.

4 Calculating statistical uncertain.

The intensity Radioactive Ion Beam in a graphite target was of 10^{10} s^{-1}.

The irradiating neutron flux is of $5.3\cdot10^{10}$ neutron/cm^2·s.

The gamma activity of the activated $\mathbf{X^{A+1}}$ nuclide is measured.

The γ- background count rate of activity of the unstable $\mathbf{X^{A}}$ nuclides shoud be less then the maximum count rate c_{max} for this detector (HPGe or BriLanCe ($LaBr_3$:Ce). The instrumental, cosmic and Compton background from the higher gamma level are taken into account.

The calculate statistical uncertain of the MACS measuring by the activation method are given in Table 2.

Tab. 2 The calculate statistical uncertain of the MACS measuring by the activation method.

Implanted unstable nuclide $\mathbf{X^{A}}$	Implanted tame	The mass of nuclide $\mathbf{X^{A}}$	Time of irradiation	Activated nuclide $\mathbf{X^{A+1}}$	Time of measurement statistics uncertain
^{90}Sr ($\tau_{1/2}$ = 29 y)	14 day	1.8 μg $1.21\cdot10^{16}$ atoms	12 h	^{91}Sr $\xrightarrow{\beta}$ ^{91}Y ($\tau_{1/2}$ = 10 h)	1 d **2%**
^{94}Nb ($\tau_{1/2} = 2\cdot10^4$ y)	1 day	1.3 μg $0.86\cdot10^{15}$ atoms	14 day	^{95}Nb $\xrightarrow{\beta}$ ^{95}Mo ($\tau_{1/2}$ = 10 h)	40 d **2%**
^{99}Tc ($\tau_{1/2} = 2\cdot10^5$ y)	14 day	2.0 μg $1.21\cdot10^{16}$ atoms	3 min	^{100}Tc $\xrightarrow{\beta}$ ^{95}Ru ($\tau_{1/2}$ = 16 s)	1 min **1%**
^{104}Ru ($\tau_{1/2}$ = 45 s)	14 day	2.1 μg $1.21\cdot10^{16}$ atoms	36 h	^{105}Ru $\xrightarrow{\beta}$ ^{105}Pd ($\tau_{1/2}$ = 35 h)	3 day **5%**

^{116}Cd ($\tau_{1/2} = 3 \cdot 10^{19}$ y)	14 day	2.3 μg $1.21 \cdot 10^{16}$ atoms	3 h	$^{117}Cd \xrightarrow{\beta} {}^{117}In$ ($\tau_{1/2} = 2.5$ h)	3 h **1%**
$^{114}In^{m}$ ($\tau_{1/2} = 50$ d)	1 day	1.6 μg $0.86 \cdot 10^{15}$ atoms	5 h	$^{115}In \xrightarrow{\beta} {}^{115}Sn$ ($\tau_{1/2} = 10^{14}$ y)	5 h **1%**
^{115}In ($\tau_{1/2} = 10^{14}$ y)	14 day	2.3 μg $1.21 \cdot 10^{16}$	15 s	$^{116}In \xrightarrow{\beta} {}^{116}Sn$ ($\tau_{1/2} = 16$ s)	15 s **3%**
^{124}Sb ($\tau_{1/2} = 60$ d)	1 day	$0.86 \cdot 10^{15}$ at.	12 day	$^{125}Sb \xrightarrow{\beta} {}^{115}Tl$ ($\tau_{1/2} = 2.7$ y)	1 y **3%**
^{129}I ($\tau_{1/2} = 10^{7}$ y)	14 day	$1.21 \cdot 10^{16}$ at.	12 h	$^{130}I \xrightarrow{\beta} {}^{130}Xe$ ($\tau_{1/2} = 2.7$ y)	12 h **1%**
^{134}Cs ($\tau_{1/2} = 2$ y)	6 h	$2.16 \cdot 10^{14}$ at.	1 h	$^{135}Cs \xrightarrow{\beta} {}^{135}Ba$ ($\tau_{1/2} = 10^{6}$y)	3 h **2%**
^{135}Cs ($\tau_{1/2} = 10^{6}$ y)	14 day	$1.21 \cdot 10^{16}$ at.	14 h	$^{136}Cs \xrightarrow{\beta} {}^{136}Ba$ ($\tau_{1/2} = 13$ d)	1 d **1%**
^{136}Cs ($\tau_{1/2} = 13$ d)	14 day	$8.56 \cdot 10^{15}$ at.	14 h	$^{137}Cs \xrightarrow{\beta} {}^{137}Ba$ ($\tau_{1/2} = 30$ y)	14 d **4%**
^{137}Cs ($\tau_{1/2} = 30$ y)	14 day	$1.21 \cdot 10^{16}$ at.	1 h	$^{138}Cs \xrightarrow{\beta} {}^{138}Ba$ ($\tau_{1/2} = 33$ min)	1 d **1%**
^{143}Ce ($\tau_{1/2} = 33$ h)	14 day	$1.19 \cdot 10^{16}$ at.	14 h	$^{144}Ce \xrightarrow{\beta} {}^{144}Pr$ ($\tau_{1/2} = 285$ d)	300 d **5%**
^{144}Ce ($\tau_{1/2} = 285$ d)	14 day	$1.21 \cdot 10^{16}$ at.	5 min	$^{145}Ce \xrightarrow{\beta} {}^{145}Pr$ ($\tau_{1/2} = 3$ min)	5 min **2%**
^{143}Pr ($\tau_{1/2} = 14$ d)	14 day	$8.64 \cdot 10^{15}$ at.	30 min	$^{144}Pr \xrightarrow{\beta} {}^{144}Nd$ ($\tau_{1/2} = 17$ min)	30 min **1%**
^{149}Pm ($\tau_{1/2} = 53$ h)	3 day	$1.68 \cdot 10^{15}$ at.	3 h	$^{150}Pm \xrightarrow{\beta} {}^{150}Sm$ ($\tau_{1/2} = 2$ h)	3 h **2%**
^{160}Tb ($\tau_{1/2} = 72$ d)	6h	$2.16 \cdot 10^{14}$ at.	7 d	$^{161}Tb \xrightarrow{\beta} {}^{161}Dy$ ($\tau_{1/2} = 6.8$ d)	7 d **3%**
^{161}Tb ($\tau_{1/2} = 6.8$ d)	6h	$2.16 \cdot 10^{14}$ at.	20 min	$^{162}Tb \xrightarrow{\beta} {}^{162}Dy$ ($\tau_{1/2} = 7.6$ min)	20 min **1%**
^{166}Ho ($\tau_{1/2} = 27$ h)	1 day	$8.5 \cdot 10^{14}$ at.	3 h	$^{167}Ho \xrightarrow{\beta} {}^{167}Er$ ($\tau_{1/2} = 3$ h)	3 h **1%**
^{181}Hf	14 day	$1.2 \cdot 10^{16}$ at.	12 day	$^{182}Hf \xrightarrow{\beta} {}^{182}Ta$	12 day

($\tau_{1/2}$ = 44 d) ($\tau_{1/2}$ = 9 10^6 y) **2%**

Formulas for calculating:

A namber of atoms of implanted X^A isotope befor irradiating:

$$N_0 = I_0 \times T^0_{1/2} \times (1 - \exp(-0.693\, t_{impl} / T^0_{1/2}))/0.693$$

The γ– and β- activity of the implanted X^A isotope befor irradiating:

$$A^0_\gamma = I_0 \times (1 - \exp(-0.693\, t_{impl} / T^0_{1/2}) \times I^0_\gamma$$

$$A^0_\beta = I_0 \times (1 - \exp(-0.693\, t_{impl} / T^0_{1/2}) \times I^0_\beta$$

I_0 - intensity of the ion implantation (10^{10} p/s)

t_{impl} –time of the implantation

$T^0_{1/2}$ – half-life of implantated ions

I^0_γ - intensity of the gamma rays from the decay of the one implantated X^A ion

I^0_β - intensity of the beta particles from the decay of the one implantated X^A ion

The γ– and β- activity of the X^{A+1} isotope after irradiating neutrons:

if $T^0_{1/2} \neq T^1_{1/2}$:

$$A^1_\gamma = I^1_\gamma \times I_1 \times \sigma \times N_0 \times (\exp(-0.693\, t_{irrad}/T^0_{1/2}) - \exp(-0.693\, t_{irrad}/T^1_{1/2})) \times T^0_{1/2} / (T^0_{1/2} - T^1_{1/2})$$

$$A^1_\beta = I^1_\beta \times I_1 \times \sigma \times N_0 \times (\exp(-0.693\, t_{irrad}/T^0_{1/2}) - \exp(-0.693\, t_{irrad}/T^1_{1/2})) \times T^0_{1/2} / (T^0_{1/2} - T^1_{1/2})$$

if $T^0_{1/2} \approx T^1_{1/2}$:

$$A^1_\gamma = I^1_\gamma \times I_1 \times \sigma \times N_0 \times \exp(-0.693\, t_{irrad}/T^1_{1/2}) \times 0.693 \times t_{irrad}/T^1_{1/2}$$

$$A^1_\beta = I^1_\gamma \times I_1 \times \sigma \times N_0 \times \exp(-0.693\, t_{irrad}/T^1_{1/2}) \times 0.693 \times t_{irrad}/T^1_{1/2}$$

I_1 - intensity of the neutrons ($5.3 \cdot 10^{10}$ n/cm^2·s)

t_{irrad} –time of the irradiation

$T^1_{1/2}$ – half-life of the X^{A+1} isotope atom

I^1_γ - intensity of the gamma rays from the decay of the one X^{A+1} isotope atom

I^1_β - intensity of the beta particles from the decay of the one X^{A+1} isotope atom

σ - the extrapolation Maxwellian-averaged cross sections of the X^A isotope at the kT=30 keV.

The γ– and β- activity of the implanted X^A isotope after cooling, befor measurement:

$$A^{0c}_\gamma = A^0_\gamma \times \exp(-0.693(t_{irrad} + t_{cool})/T^0_{1/2})$$ t_{cool} –time of cooling

$$A^{0c}_\beta = A^0_\beta \times \exp(-0.693\, t_{irrad} + t_{cool})/T^0_{1/2})$$

This activity is background. This count rate should be less then the maximum count rate for the detector c_{max} .

The counting statistics of the registered γ– and β- activity of the decayed atoms of X^{A+1} isotope in the time of measurement: t_{cool} –time of cooling

$$C_1{}^m{}_\gamma = \Omega \times \varepsilon_\gamma \times A^1_\gamma \times \exp(-0.693\, t_{cool}/T^1_{1/2}) \times (1 - \exp(-0.693\, t_{meas}/T^1_{1/2})) \times T^1_{1/2}/0.693$$

$$C_1{}^m{}_\beta = \Omega \times \varepsilon_\beta \times A^1_\beta \times \exp(-0.693\, t_{cool}/T^1_{1/2}) \times (1 - \exp(-0.693\, t_{meas}/T^1_{1/2})) \times T^1_{1/2}/0.693$$

$\Omega = \Omega_1 + \Omega_2$ – geometric efficiency of the detectors is $\approx \varnothing^2/16R^2$ at large distance of R between measured sample and detector (is deameter of ∅) should be placed plastic to absorb electron of the β-decay .

$\varepsilon = \varepsilon_1 = \varepsilon_2$; ε_γ = efficiency **FEPE** of the detector; $\varepsilon_\beta \sim (E^1_\beta - E_b)/E^1_\beta$, E_b - threshold energy ($\sim E^0_\beta$ maximum)

A counting statistics of the registration gamma rays in the coincidence mode is:

$$C_{\gamma\gamma}{}^{cc} = C_1{}^m{}_\gamma \times \Omega \times \varepsilon$$

The registered background of the γ– and β- activity of the decayed atoms of X^A isotope in the time of measurement:

$\mathbf{C_f^m{}_\gamma = \Omega \times \varepsilon^f{}_\gamma \times I^f_\gamma \times N^m{}_0 = \Omega \times \varepsilon^f{}_\gamma \times A^{0c}{}_\gamma \times T^0{}_{1/2}/0.693}$

$\mathbf{C_f^m{}_\beta = \Omega \times \varepsilon^f{}_\beta \times I^f_\beta \times N^m{}_0 = \Omega \times \varepsilon^f{}_\beta \times A^{0c}{}_\beta \times T^0{}_{1/2}/0.693}$

$\varepsilon^f{}_\gamma \approx \Delta E_\gamma / E^0{}_\gamma$

$\varepsilon^f{}_\beta \sim (E^1{}_\beta - E^0{}_\beta) / E^1{}_\beta$

ΔE- energy resolution of the detector

τ_{cc} - resoulion time of set up of two detector (τ_{cc} =1ns)

I^f_γ – intensity of bacgraund gamma rays

In the coincidence mode count rate of the γ – and β -background from X^A decay is reduce to:

$\mathbf{C_f^{cc} = 2 \times C_0^m{}_\gamma \times A_\gamma{}^0 \times \tau_{cc} \times \Omega \times \varepsilon^f{}_\gamma}$

$\mathbf{C_f^{cc} = 2 \times C_0^m{}_\beta \times A_\gamma{}^0 \times \tau_{cc} \times \Omega \times \varepsilon^f{}_\beta}$

References

1. N. Patronis, S. Dababneh, et al. Phys. Rev. **C 69** (2004) 025803.
2. F. Gramegna, A. Andrighetto, et al. Acta Phys. Polon. **B 38** (2007) 1157.
3. W. Ratynski and F. Käppeler, Phys. Rev. C **37**, (1988) 595.
4. Alekseev A.A., Bergman A.A. et al. ISINN-12, Dubna (2004) 237.

.